

Odd and even photon-subtracted two-mode squeezed vacuum states

Ananga Mohan Datta,¹ Kurt Busch,^{1,2} and Armando Perez-Leija³

¹*Humboldt-Universität zu Berlin, Institut für Physik,
AG Theoretische Optik & Photonik, Newtonstr. 15, 12489 Berlin, Germany*

²*Max-Born-Institut, Max-Born-Str. 2A, 12489 Berlin, Germany*

³*CREOL, The College of Optics and Photonics, University of Central Florida, Orlando, Florida 32816, USA*

(Dated: December 11, 2024)

Photon-subtracted two-mode squeezed vacuum states, a significant quantum resource, exhibit intricate correlations and unique quantum properties. In this work, we propose a theoretical yet experimentally feasible model to engineer these states using a waveguide trimer. Our study uncovers distinct characteristics of the photon-subtracted state depending on whether an even or odd number of photons is extracted, shedding light on the subtle relationship between quantum state manipulation and the parity of the number of subtracted photons. Furthermore, our integrated device facilitates the generation of multiphoton states with tunable correlations, offering significant potential for applications in quantum-enhanced technologies.

Sculpting the quantum and statistical properties of light is a key milestone in the development of quantum-optical information technology [1]. As a matter of fact, most of such technologies rely on state preparation that requires the engineering of quantum correlations between multiple photons distributed among different modes of the systems in question [2]. Admittedly, the generation of quantum correlated multiphoton wavepackets can be achieved using linear optical schemes [3] in combination with nonlinear light sources [4]. In this context, the notion of photon subtraction has emerged as a pragmatic method for the generation of highly correlated multiphoton states [5–7]. Its essence consists in deliberately removing a number of photons from a quantum light source, and counterintuitively, this procedure can transform Gaussian states into non-Gaussian ones endowed with enhanced mean photon numbers and appealing nonclassical properties [8]. Furthermore, photon subtraction is crucial for generating high-fidelity Gottesman-Kitaev-Preskill states, which serve as important resources for error correction and robust quantum computing in continuous-variable systems [9, 10]. Over the years, the non-classicality of zero-photon, single-photon, and multi-photon subtracted states from single-mode radiation fields has been the focus of several investigations [8, 11, 12]. And more recently, such photon-subtraction practice has been extended to multimode fields, e.g., multimode thermal states [13], two-mode squeezed thermal states [14], and two-mode squeezed vacuum states (TMSVSs) [15, 16]. Interestingly, the application of photon-subtraction to TMSVSs has recently yielded to the observation of highly-correlated multiphoton states comprising up to ten photons [7]. This latter achievement, combined with the fact that TMSVSs are the most accessible highly-entangled multiphoton states [4], makes photon-subtracted TMSVS extremely appealing for quantum-enhanced applications, e.g., quantum interferometry [5], teleportation protocols [17], quantum illumination [6], and enhancement of quantum entangle-

ment [18, 19].

In practice, the photon subtraction scheme, applied to a general TMSVS, $|r\rangle = \sqrt{1 - |r|^2} \sum_{n=0}^{\infty} r^n |n\rangle_a |n\rangle_b$, with the squeeze parameter r , is implemented using two beamsplitters placed in the paths traced out by the modes. The state characterization is done using four photon-number resolving (PNR) detectors, two for counting the reflected photons (subtracted photons) and two to register the transmitted photons, i.e., the photons left in the initial beams [7]. Here are two possible subtraction scenarios: i) the symmetric case when the same number of photons is subtracted from each beam, and ii) the asymmetric one when a different number of photons is subtracted. Mathematically, both subtraction processes are described by the transformation $\hat{a}^l \hat{b}^m |r\rangle = \mathcal{N}^{-1} \sqrt{1 - |r|^2} \sum_n r^n n! ((n-l)(n-m)!)^{-1/2} |n-l\rangle_a |n-m\rangle_b$, where the sum runs from $n = l$ ($n = m$) if $l > m$ ($m > l$), \mathcal{N} is a normalization constant, and \hat{a}, \hat{b} are the bosonic annihilation operators for modes a and b , respectively. Hence, both subtraction schemes render infinite superpositions of joint photon number states of the type $|m\rangle_a |m\rangle_b$ or $|m\rangle_a |n\rangle_b$ depending on the symmetry of the subtraction process.

In this work, we investigate a complementary photon-subtraction scheme that arises when both modes comprised in the TMSVS become equally coupled to a common channel in such a way that when measuring the number of photons hopping into this channel, we will know the number of photons being extracted from the beams, but we will not be able to distinguish from which beam the photons arriving at the detector emanated. Interestingly, this lack of information allows the system to inhabit a space of infinite superpositions of joint photon number states of the type $|m\rangle_a |n\rangle_b + |n\rangle_a |m\rangle_b + |m\rangle_a |m\rangle_b$ or $|m\rangle_a |n\rangle_b + |n\rangle_a |m\rangle_b$ depending on the parity (evenness or oddness) of the number of extracted photons. Furthermore, to place our findings on solid ground, we propose a versatile experimental scheme based on an integrated waveguide trimer [20], where the TMSVSs

are coupled into the two outermost waveguides, and the photon-subtraction is achieved by measuring the photons that tunnel into the central channel. Importantly, this type of trimer can be implemented using current technology, e.g femtosecond-laser-writing techniques [21], silicon nanowires [22], or even lithium niobate (LiNbO₃)-based platform [23].

We begin with the evolution of the quantized electromagnetic fields in a waveguide trimer, described by the Heisenberg equation for the bosonic creation operators \hat{a}^\dagger , \hat{b}^\dagger , and \hat{c}^\dagger , assuming equal propagation constants β among the three waveguides, is expressed as follows:

$$i \frac{d}{dz} \begin{pmatrix} \hat{a}^\dagger(z) \\ \hat{b}^\dagger(z) \\ \hat{c}^\dagger(z) \end{pmatrix} = \begin{pmatrix} \beta & \kappa & 0 \\ \kappa & \beta & \kappa \\ 0 & \kappa & \beta \end{pmatrix} \begin{pmatrix} \hat{a}^\dagger(z) \\ \hat{b}^\dagger(z) \\ \hat{c}^\dagger(z) \end{pmatrix}. \quad (1)$$

Here, κ represents the coupling coefficient between adjacent waveguides in the system and z signifies the propagation distance. Ignoring the propagation constant since it is equal for the three waveguides, the general solution for the coupled equation system can be written as

$$\begin{pmatrix} \hat{a}^\dagger(z) \\ \hat{b}^\dagger(z) \\ \hat{c}^\dagger(z) \end{pmatrix} = U(z) \begin{pmatrix} \hat{a}^\dagger(0) \\ \hat{b}^\dagger(0) \\ \hat{c}^\dagger(0) \end{pmatrix}, \quad (2)$$

where the elements of the evolution matrix $U(z)$ is given by:

$$U(z) = e^{i\beta z} \begin{pmatrix} \frac{1}{2} + \frac{1}{2} \cos \Theta & -\frac{i \sin \Theta}{\sqrt{2}} & -\frac{1}{2} + \frac{1}{2} \cos \Theta \\ -\frac{i \sin \Theta}{\sqrt{2}} & \cos \Theta & -\frac{i \sin \Theta}{\sqrt{2}} \\ -\frac{1}{2} + \frac{1}{2} \cos \Theta & -\frac{i \sin \Theta}{\sqrt{2}} & \frac{1}{2} + \frac{1}{2} \cos \Theta \end{pmatrix}, \quad (3)$$

where $\Theta = \sqrt{2}\kappa z$. Considering the configuration illustrated in Fig. 1, the waveguides a and c are injected with a TMSVS, while waveguide b has the vacuum state as input. Photons are subtracted from the central waveguide b using a PNR detector at its output, and the resulting state is analyzed using PNR detectors at waveguides a and c , all assumed to have quantum efficiency η . Initially, we examine the state assuming perfect PNR detection ($\eta = 1$). Subsequently, we briefly assess the impact of small imperfections in the PNR detection process.

Under this excitation scheme for the waveguide trimer, the input state can be expressed as $|\psi_{\text{in}}\rangle = (1 - |r|^2)^{\frac{1}{2}} \sum_{l=0}^{\infty} r^l |l\rangle_a |0\rangle_b |l\rangle_c$. To analyze the output state, we choose the propagation distance z to optimize light transmission to the outermost waveguides while maintaining a feasible probability of photon subtraction from the central waveguide. Specifically, we set the intensity ratio $I_{\text{cen}}/I_{\text{out}} = 10/90$, meaning that 10% of the total intensity is distributed across the central waveguide (I_{cen}) and 90% across the outermost waveguides (I_{out}). Adjusting this intensity ratio, the corresponding propagation distance is determined as $z = z_f \approx 0.23/\kappa$. Using the transformation described in Eq. (2), we calculate

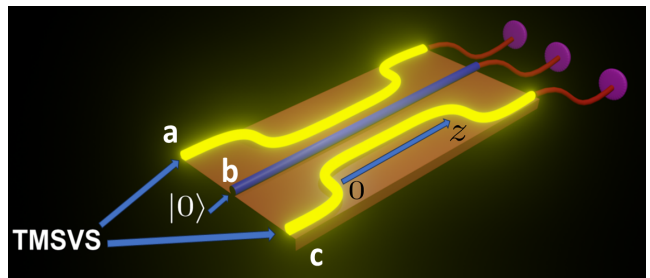


FIG. 1. The schematic setup depicts a waveguide trimer utilized for photon subtraction from TMSVS. TMSVS are injected into the outermost waveguides, while photons are subtracted from the central port b using PNR detector. The resulting photon-subtracted TMSVS is analyzed using two PNR detectors placed at ports a and c .

the output state at the propagation distance z_f , given by $|\psi_{\text{out}}\rangle = U(z_f) |\psi_{\text{in}}\rangle$, where $U(z_f)$ is the evolution matrix calculated at the particular propagation distance $z = z_f$. The photon-subtracted state, denoted as $\hat{\rho}_{\text{sub}}$, is then computed as $\hat{\rho}_{\text{sub}} = \text{Tr}_b(\hat{P}_b |\psi_{\text{out}}\rangle \langle \psi_{\text{out}}|)$, where, $\text{Tr}_b(\cdot)$ signifies the partial trace operation over Fock states in waveguide b . The operator \hat{P}_b stands for the positive operator-valued measure (POVM) operator for a PNR detector with a quantum efficiency η , aimed at detecting N photons in waveguide b . Specifically, $\hat{P}_b =: \frac{\eta^{\hat{n}_b}}{N!} e^{-\eta \hat{n}_b} :$, where $::$ represents the normal ordering prescription[24]. Further, \hat{n}_b represents the number operator acting on Fock basis states in waveguide b . To analyze the resulting states, we first examine the joint photon-number distribution, which characterizes the probability of detecting m photons in waveguide a and n photons in waveguide c while subtracting N photons from waveguide b . This distribution is given by:

$$\mathcal{P}_{m,n} = \left\langle : \frac{(\eta \hat{n}_a)^m}{m!} e^{-\eta \hat{n}_a} \otimes \frac{(\eta \hat{n}_c)^n}{n!} e^{-\eta \hat{n}_c} : \right\rangle \quad (4)$$

where \hat{n}_a and \hat{n}_c are number operator acting on Fock basis states in waveguides a and c , respectively. In Fig. 2, we illustrate the joint photon-number distribution, wherein zero to three photons are subtracted from the central waveguide. An interesting observation emerges in the patterns of the photon-number distribution, particularly regarding even and odd values of N . In instances of even N , the joint photon-number distribution can be expressed as superposition of the states of the type $|m\rangle_a |n\rangle_b$, $|n\rangle_a |m\rangle_b$, and $|m\rangle_a |m\rangle_b$. Consequently, the distribution features both diagonal and off-diagonal elements, with a single peak along the diagonals, as illustrated in Fig. 2(c). The special case of $N = 0$ represents zero photon subtraction from each of the beams, resulting in a photon-number distribution plot with only diagonal elements, as shown in Fig. 2(a). This form arises because of the nature of photon subtraction. The first two terms, $|m\rangle_a |n\rangle_b$ and $|n\rangle_a |m\rangle_b$, result from asymmetric

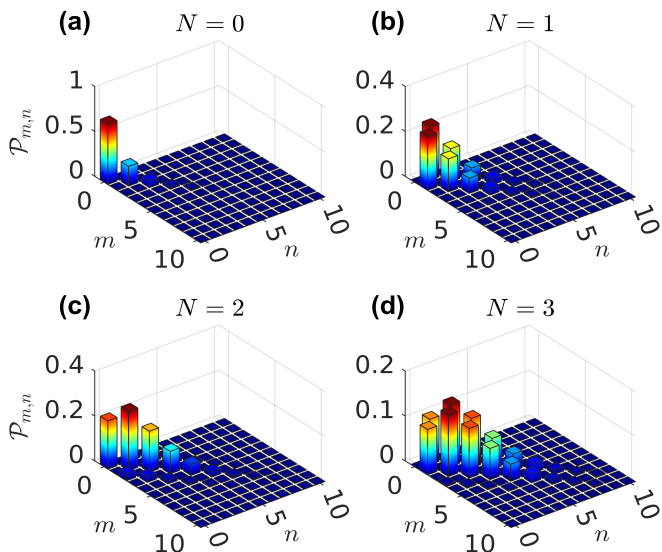


FIG. 2. The joint photon-number distributions for the photon-subtracted TMSVS are analyzed for $|r| = 0.6$, $z = z_f$, and $\eta = 1$. Figures (a), (b), (c), and (d) illustrate the distributions for subtracting zero ($N = 0$), one ($N = 1$), two ($N = 2$), and three ($N = 3$) photons from the central port, respectively.

photon subtraction, where different numbers of photons are subtracted from the two beams of the TMSVS. The third term, $|m\rangle_a |m\rangle_b$, is due to symmetric photon subtraction, where the same number of photons is subtracted from both beams. Therefore, when N is even, it indicates a scenario where photons are subtracted either symmetrically or asymmetrically, without specifying precisely which mode undergoes photon extraction. Conversely, for odd values of N , the joint photon-number distribution consists of a superposition of the states $|m\rangle_a |n\rangle_b$ and $|n\rangle_a |m\rangle_b$, resulting in only off-diagonal elements. This occurs due to the solely asymmetric photon subtraction, again without knowledge on which beam the photons are taken from. The absence of diagonal elements, due to the lack of states of the form $|m\rangle_a |m\rangle_b$, creates a central nodal line in the distribution with two peaks located on either side of this line, as shown in Figs. 2(b) and 2(d). Significantly, the peak(s) of the distributions for even (odd) values of N show a noticeable shift towards higher photon numbers as N increases, indicating an overall increase in the average photon number. This increment can be directly verified by computing the average photon number in one of the modes, expressed as $\langle \hat{n} \rangle = \sum_{m=0}^{\infty} m \mathcal{P}_{m,n}$, where the total average photon number is $2 \langle \hat{n} \rangle$. In Fig. 3, we display the total average photon number $2 \langle \hat{n} \rangle$ with the squeeze parameter $|r|$ for different values of N . Interestingly, when considering lower values of $|r|$, the average photon number of the state resulting from an odd number of photon subtractions exceeds that from subtracting an even number of

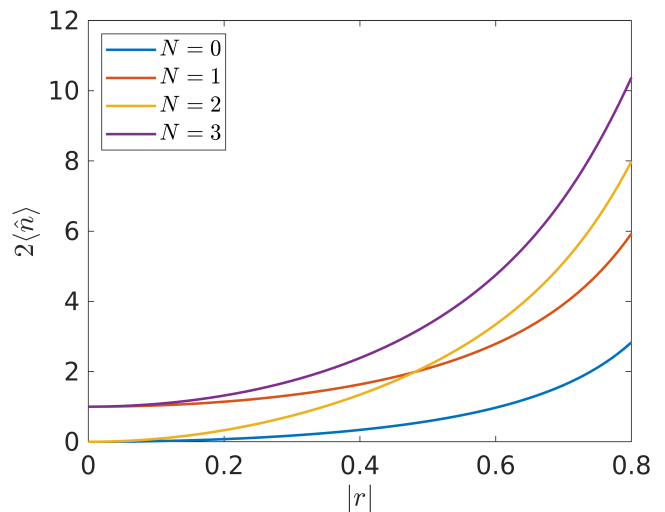


FIG. 3. The total mean photon number of a photon-subtracted TMSVS is examined as a function of $|r|$ for $N = 0, 1, 2$, and 3 at a propagation distance of $z = z_f$, assuming a quantum efficiency of $\eta = 1$.

photons from the central waveguide. However, beyond a certain value of $|r|$, the average photon number increases as N increases. This behavior is reminiscent of that observed in Schrödinger-cat-like states, as previously discussed [25].

Another intriguing feature of photon-subtracted TMSVSs is the presence of the strong correlations [7]. One natural approach to explore the correlations among the generated photon wavepackets at the output is through the analysis of the matrix of moments [26]. Theoretical discussions [27] and experimental demonstrations utilizing PNR detectors [7] and click detectors [28] have highlighted nonclassical correlations using the framework of the matrix of moments. By defining the operator $\hat{m}_{a(c)} = \eta \hat{n}_{a(c)}$, one can write the joint moments $\langle : \hat{m}_a^u \otimes \hat{m}_c^v : \rangle$ in terms of the photon-number distribution $\mathcal{P}_{m,n}$, and subsequently construct a matrix of moments of any order. In particular, studying the behavior of the second-order matrix of moments enables us to analyze the correlations, denoted as

$$M = \begin{pmatrix} \langle : \hat{m}_a^0 \hat{m}_c^0 : \rangle & \langle : \hat{m}_a^1 \hat{m}_c^0 : \rangle & \langle : \hat{m}_a^0 \hat{m}_c^1 : \rangle \\ \langle : \hat{m}_a^1 \hat{m}_c^0 : \rangle & \langle : \hat{m}_a^2 \hat{m}_c^0 : \rangle & \langle : \hat{m}_a^1 \hat{m}_c^1 : \rangle \\ \langle : \hat{m}_a^0 \hat{m}_c^1 : \rangle & \langle : \hat{m}_a^1 \hat{m}_c^1 : \rangle & \langle : \hat{m}_a^0 \hat{m}_c^2 : \rangle \end{pmatrix}. \quad (5)$$

As previously shown in [7], the presence of nonclassical correlations is indicated by $\text{Det}(M) < 0$. Conversely, a positive value of the determinant denotes classical correlations. We provide some details on computing the second-order matrix of moments in the supplemental material. In Fig. 4, $\text{Det}(M)$ is plotted against $|r|$ for different N values. Notably, the uncertainty regarding which beam the photons are extracted from leads to intriguing observations about the nature of the correlations.

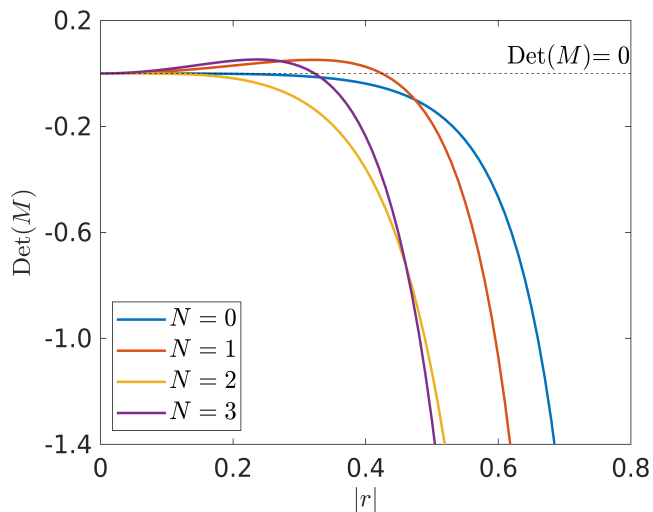


FIG. 4. The determinant of the second-order matrix of moments M , is examined as a function of $|r|$ to quantify the correlations between the two output modes of a photon-subtracted TMSVS. This analysis is conducted for values of $N = 0, 1, 2$, and 3 at a propagation distance of $z = z_f$, with the assumption of a quantum efficiency of $\eta = 1$. The black dotted line represent $\text{Det}(M) = 0$.

For odd values of N , we observe classical correlations at small values of the parameter $|r|$, while even N values predominantly show nonclassical correlations. In other words, we observe destruction of quantum coherence in the photon-subtracted state for odd N at low squeeze parameters [29]. At higher values of $|r|$, there is an enhancement of nonclassical correlations with increasing N . This distinct feature, where different correlations emerge at small squeeze parameters, is reminiscent of the properties observed in two-mode Schrödinger cat states [30, 31]. Even and odd two-mode coherent states exhibit distinct nonclassical characteristics, especially at low coherence amplitudes [31]. In this context, our protocol is useful for generating two-mode Schrödinger-cat states in an integrated platform.

Finally, we investigate the effect of imperfections from PNR detectors on the correlations by computing the determinant of the second-order matrix of moments for $N = 0, 1, 2$, and 3 , considering various values of the parameter $|r|$. We assume a quantum efficiency of $\eta = 0.8$ for each detector. From the data presented in Table I, we note that the distinctive correlation patterns between even and odd numbers of subtracted photons endure, despite imperfections in the detection process. It is important to remark that this distinct nature in correlations of the generated multiphoton states has not been observed in previous photon-subtraction protocols [5–7, 15, 17, 18].

In conclusion, we have proposed and analyzed a waveguide trimer to engineer photon-subtracted TMSVS, ef-

TABLE I. The determinant of the second-order matrix of moments M , is calculated for various values of $|r|$ to examine the impact of imperfections stemming from the PNR detection process, which are on the order of 10^{-3} . This analysis is conducted for $z = z_f$ and $\eta = 0.8$.

$ r $	$N = 0$	$N = 1$	$N = 2$	$N = 3$
0.2	-0.62	1.71	-7.49	8.48
0.3	-3.79	9.35	-40.67	8.18

fectively reducing the number of required PNR detectors to three, compared to the four PNR detectors typically needed in the conventional photon subtraction process from twin beams [7, 15, 16]. Monitoring a single port for photon subtraction allows us to observe photon-number distributions at the outermost waveguides. Notably, we observe distinct characteristics in the photon-subtracted state when retrieving an odd or even number of photons from the central waveguide. Specifically, we find that the nature of correlations exhibit a clear dependence on the parity of the extracted photons, particularly at low values of the squeeze parameter, resembling the behavior of two-mode cat states. We have shown that the device performance remains robust even with imperfect detectors in operation. Moreover, our framework allows for a detailed analysis of specific settings with particular imperfections [7, 15, 32]. Furthermore, we present a scheme to engineer multiphoton states with tunable correlations using integrated devices. This contribution advances multiphoton integrated-optics protocols and provides a practical framework for generating and manipulating complex quantum states, enhancing the capabilities of integrated quantum photonics [33–36].

Our proposed model holds practical significance in various correlation-based schemes. For example, the creation of multiphoton states with controlled correlations through photon subtraction could notably enhance applications in quantum illumination [37], as discussed in [6]. Additionally, previous studies have showcased the implementation of Boson sampling through the photon subtraction method [38]. In this regards, our device will be useful to increase the robustness of Boson sampling in integrated photonics circuits [39]. Notably, our proposed scheme facilitates both symmetric and asymmetric photon subtraction, providing versatility tailored to the specific input state, as discussed in prior works [6, 19].

In this work, our focus has been on investigating photon-subtracted TMSVS using three PNR detectors. However, PNR detectors are typically characterized by their large size, slow response times, high cost, and complex operation [40]. Conversely, click detectors offer the advantage of easy integration into quantum optics setups and experimental systems, making them a practical choice for a variety of applications [28]. An intriguing direction for future research would be to im-

plement a multiple-click detection scheme to analyze photon-subtracted two-mode states, thereby simplifying the experimental setup.

Acknowledgment—The authors acknowledge financial support by the Leibniz Association within the Leibniz Collaborative Excellence Program (Project ID K266/2019, On-chip Laser-written Photonic Circuits for Classical and Quantum Applications (LAPTON)). A.M.D. and K.B. acknowledge funding by the German Research Foundation (DFG) in the framework of the Collaborative Research Center (CRC) 1375 (Project ID 398816777 - Project A06)

-
- [1] A. Datta, L. Zhang, N. Thomas-Peter, U. Dorner, B. J. Smith, and I. A. Walmsley, Quantum metrology with imperfect states and detectors, *Phys. Rev. A* **83**, 063836 (2011).
- [2] F. Dell’Anno, S. De Siena, and F. Illuminati, Multiphoton quantum optics and quantum state engineering, *Physics Reports* **428**, 53 (2006).
- [3] E. Knill, R. Laflamme, and G. J. Milburn, A scheme for efficient quantum computation with linear optics, *Nature* **409**, 46 (2001).
- [4] A. F. Abouraddy, B. E. A. Saleh, A. V. Sergienko, and M. C. Teich, Role of entanglement in two-photon imaging, *Phys. Rev. Lett.* **87**, 123602 (2001).
- [5] R. Carranza and C. C. Gerry, Photon-subtracted two-mode squeezed vacuum states and applications to quantum optical interferometry, *J. Opt. Soc. Am. B* **29**, 2581 (2012).
- [6] L. Fan and M. S. Zubairy, Quantum illumination using non-gaussian states generated by photon subtraction and photon addition, *Phys. Rev. A* **98**, 012319 (2018).
- [7] O. S. Magaña-Loaiza, R. de J. León-Montiel, A. Perez-Leija, A. B. U’Ren, C. You, K. Busch, A. E. Lita, S. W. Nam, R. P. Mirin, and T. Gerrits, Multiphoton quantum-state engineering using conditional measurements, *npj Quantum Inf* **5**, 80 (2019).
- [8] A. Zavatta, V. Parigi, M. S. Kim, and M. Bellini, Subtracting photons from arbitrary light fields: experimental test of coherent state invariance by single-photon annihilation, *New J. Phys.* **10**, 123006 (2008).
- [9] M. Eaton, R. Nehra, and O. Pfister, Non-gaussian and gottesman–kitaev–preskill state preparation by photon catalysis, *New Journal of Physics* **21**, 113034 (2019).
- [10] K. Takase, F. Hanamura, H. Nagayoshi, J. E. Bourassa, R. N. Alexander, A. Kawasaki, W. Asavanant, M. Endo, and A. Furusawa, Generation of flying logical qubits using generalized photon subtraction with adaptive gaussian operations, *Phys. Rev. A* **110**, 012436 (2024).
- [11] C. M. Nunn, J. D. Franson, and T. B. Pittman, Modifying quantum optical states by zero-photon subtraction, *Phys. Rev. A* **105**, 033702 (2022).
- [12] M. Endo, R. He, T. Sonoyama, K. Takahashi, T. Kashiwazaki, T. Umeki, S. Takasu, K. Hattori, D. Fukuda, K. Fukui, K. Takase, W. Asavanant, P. Marek, R. Filip, and A. Furusawa, Non-gaussian quantum state generation by multi-photon subtraction at the telecommunication wavelength, *Opt. Express* **31**, 12865 (2023).
- [13] K. G. Katamadze, G. V. Avosopiants, N. A. Bogdanova, Y. I. Bogdanov, and S. P. Kulik, Multimode thermal states with multiphoton subtraction: Study of the photon-number distribution in the selected subsystem, *Phys. Rev. A* **101**, 013811 (2020).
- [14] X.-G. Meng, K.-C. Li, J.-S. Wang, X.-Y. Zhang, Z.-T. Zhang, Z.-S. Yang, and B.-L. Liang, Continuous-variable entanglement and wigner-functionnegativity via adding or subtracting photons, *Ann. Phys.* **532**, 1900585 (2020).
- [15] K. Thapliyal, J. Peřina, O. H. Jr., V. Michálek, and R. Machulka, Experimental characterization of multimode photon-subtracted twin beams, *Phys. Rev. Research* **6**, 013065 (2024).
- [16] J. Peřina, K. Thapliyal, O. Haderka, V. Michálek, and R. Machulka, Sub-poissonian twin beams, *Optica Quantum* **2**, 148 (2024).
- [17] T. Opatrny, G. Kurizki, and D.-G. Welsch, Improvement on teleportation of continuous variables by photon subtraction via conditional measurement, *Phys. Rev. A* **61**, 032302 (2000).
- [18] A. Ourjoumtsev, A. Dantan, R. Tualle-Brouiri, and P. Grangier, Increasing entanglement between gaussian states by coherent photon subtraction, *Phys. Rev. Lett.* **98**, 030502 (2007).
- [19] T. J. Bartley, P. J. D. Crowley, A. Datta, J. Nunn, L. Zhang, and I. Walmsley, Strategies for enhancing quantum entanglement by local photon subtraction, *Phys. Rev. A* **87**, 022313 (2013).
- [20] A. Perez-Leija, J. C. Hernandez-Herrejón, H. Moya-Cessa, A. Szameit, and D. N. Christodoulides, Generating photon-encoded w states in multiport waveguide-array systems, *Phys. Rev. A* **87**, 013842 (2013).
- [21] M. Gräfe, R. Heilmann, A. Perez-Leija, R. Keil, F. Dreisow, M. Heinrich, H. Moya-Cessa, S. Nolte, D. N. Christodoulides, and A. Szameit, On-chip generation of high-order single-photon w -states, *Nature Photon* **8**, 791 (2014).
- [22] A. Blanco-Redondo, B. Bell, D. Oren, B. J. Eggleton, and M. Segev, Topological protection of biphoton states, *Science* **362**, 568 (2018).
- [23] P. R. Sharapova, K. H. Luo, H. Herrmann, M. Reichelt, T. Meier, and C. Silberhorn, Toolbox for the design of linbo3-based passive and active integrated quantum circuits, *New Journal of Physics* **19**, 123009 (2017).
- [24] L. Mandel and E. Wolf, *Optical Coherence and Quantum Optics* (Cambridge University Press, 1995).
- [25] M. Dakna, T. Anhut, T. Opatrny, L. Knöll, and D.-G. Welsch, Generating schrödinger-cat-like states by means of conditional measurements on a beam splitter, *Phys. Rev. A* **55**, 3184 (1997).
- [26] W. Vogel, Nonclassical correlation properties of radiation fields, *Phys. Rev. Lett.* **100**, 013605 (2008).
- [27] J. Sperling, W. Vogel, and G. S. Agarwal, Correlation measurements with on-off detectors, *Phys. Rev. A* **88**, 043821 (2013).
- [28] J. Sperling, M. Bohmann, W. Vogel, G. Harder, B. Brecht, V. Ansari, and C. Silberhorn, Uncovering quantum correlations with time-multiplexed click detection, *Phys. Rev. Lett.* **115**, 023601 (2015).
- [29] A. Serafini, M. G. A. Paris, F. Illuminati, and S. D. Siena, Quantifying decoherence in continuous variable systems, *Journal of Optics B: Quantum and Semiclassical Optics* **7**, R19 (2005).
- [30] C. C. Gerry and R. Grobe, Nonclassical properties of

- correlated two-mode schrödinger cat states, *Phys. Rev. A* **51**, 1698 (1995).
- [31] B. Hackery, S. Welte, S. Daiss, A. Shaukat, S. Ritter, L. Li, and G. Rempe, Deterministic creation of entangled atom–light schrödinger-cat states, *Nature Photon* **13**, 110–115 (2019).
- [32] J. Provazník, L. Lachman, R. Filip, and P. Marek, Benchmarking photon number resolving detectors, *Opt. Express* **28**, 14839 (2020).
- [33] A. M. Datta, A. Perez-Leija, and K. Busch, Tailoring the nonclassicality of light states via mode detuning in waveguide beam splitters, *J. Opt. Soc. Am. B* **41**, 1557 (2024).
- [34] J. A. Anaya-Contreras, A. Zúñiga-Segundo, A. Perez-Leija, R. de J León-Montiel, and H. M. Moya-Cessa, Multiphoton processes via conditional measurements in the two-field interaction, *J. Opt.* **23**, 095201 (2021).
- [35] J. Wang, F. Sciarrino, A. Laing, and M. G. Thompson, Integrated photonic quantum technologies, *Nat. Photonics* **14**, 273–284 (2020).
- [36] L. Labonté, O. Alibart, V. D’Auria, F. Dautre, J. Etesse, G. Sauder, A. Martin, E. Picholle, and S. Tanzilli, Integrated photonics for quantum communications and metrology, *PRX Quantum* **5**, 010101 (2024).
- [37] S. Lloyd, Enhanced sensitivity of photodetection via quantum illumination, *Science* **321**, 1463 (2008).
- [38] J. P. Olson, K. P. Seshadreesan, K. R. Motes, P. P. Rohde, and J. P. Dowling, Sampling arbitrary photon-added or photon-subtracted squeezed states is in the same complexity class as boson sampling, *Phys. Rev. A* **91**, 022317 (2015).
- [39] J. B. Spring, B. J. Metcalf, P. C. Humphreys, W. S. Kolthammer, X.-M. Jin, M. Barbieri, A. Datta, N. Thomas-Peter, N. K. Langford, D. Kundys, J. C. Gates, B. J. Smith, P. G. R. Smith, and I. A. Walmsley, Boson sampling on a photonic chip, *Science* **339**, 798 (2013).
- [40] C. Silberhorn, Detecting quantum light, *Contemporary Physics* **48**, 143 (2007).